EFFECT OF CONE ANGLE ON PENETRATION RESISTANCE

Edward A. Nowatzki and Leslie L. Karafiath, Grumman Aerospace Corporation, Bethpage, New York

A theoretically correct 3-dimensional analysis of cone penetration using plasticity theory and the Coulomb failure criterion is presented. The differential equations of plastic equilibrium are solved numerically for an ideal uniform dry sand to show the variation of slip-line field geometry with changes in the apex angle of the cone. The results indicate that, with increasing apex angle, less soil volume is affected. The results of a series of laboratory tests are plotted to show how the value of cone index increases with increasing apex angle. The differential equations of plastic equilibrium are again solved numerically for soil and boundary conditions that correspond to those of the experiments. The results support the validity of the theory in dense sands and also demonstrate that soil compressibility affects the cone index to the extent that it no longer serves as a measure of frictional strength. For loose soils, differences in cone angles have little effect on cone index, all other conditions being equal. This condition can be identified by the use of 2 cones, one having an obtuse apex angle and the other an acute apex angle. The theoretical and experimental results are correlated to show how the theory may be used for any soil to predict the angle of internal friction.

•THE MERITS of using penetrometer data for determining soil properties have been discussed extensively (6, 9, 13). In many of these reports empirical expressions are derived purporting to relate penetration test parameters to soil properties, for example, blow count data of the standard penetration test (SPT) to the relative density of the soil being penetrated. Although most of the effort has been directed toward dynamic tests such as the SPT, some consideration has also been given to relating soil parameters to static cone penetration characteristics (18). Very little attention has been paid to a theoretical analysis of the interaction between a cone penetrometer and the failing soil during the penetration process, although there exists in the literature a well-established basis for such a study. The following paragraph presents a brief review of the pertinent contributions in the area of plasticity analysis of soil problems.

The theory of static equilibrium has been combined with the Coulomb failure criterion and applied to studies of soil bearing capacity. Prandtl (12) solved the resulting differential equation of plastic equilibrium for a strip footing on weightless soil (plane strain condition). Cox, Eason, and Hopkins (4) developed a general theory of axially symmetric plastic deformations in ideal soils and applied it to the problem of the penetration of a smooth, rigid, flat-ended circular cylinder into a semi-infinite mass of weightless soil. Drucker and Prager (5) and more recently Spencer (16) extended the theory for the plane strain case to include body forces such as soil weight and cohesion; Cox (3) and more recently Larkin (8) did the same for the axially symmetric case. In cases where the characteristic relations for the governing differential equations cannot be integrated explicitly, numerical methods are used. Sokolovskii (15) presented the most widely used procedure of numerical integration, a finite difference approximation based on the method of characteristics.

Sponsored by Committee on Foundations of Bridges and Other Structures.

Studies relating specifically to cone indentation problems are less numerous. Sneddon (14) derived a solution to the cone indentation problem within the framework of the classical theory of elasticity. Meyerhof (10) and Berezantzev (1) offered approximate solutions of the axially symmetric problem. The former applied the solution to a study of the effect of surface roughness on cone penetration; the latter investigated the use of penetrometer data to determine friction angle.

OBJECTIVE

An analysis is presented of the penetration of a perfectly rigid cone into an ideal granular soil whose strength properties are defined by the Coulomb failure criterion. Plastic stress states are considered to be symmetric with the central axis of a right circular cone. A purely frictional soil is assumed so that local pore-pressure buildup may be neglected. This ensures that failure occurs in shear zones rather than along a single failure surface. In the model used in the analysis, the limit load, obtained from a solution that satisfies the basic differential equations of plasticity and the boundary stress condition, is considered a lower bound (5).

SCOPE

This study is arranged in the following order: The variables are identified and defined, the governing equations of plastic equilibrium for the axially symmetric case are given, and the limitations of the present investigation are discussed. The major results obtained from the theory within those limitations are presented and discussed with reference to experimental data. Conclusions are drawn at this point in the analysis. Finally, the results of this study are summarized, and remarks are made concerning them and their relation to future research in this area.

NOTATION

The quantities defining the geometry of the problem are shown in Figure 1. The notation is as follows:

- A_o = area of cone base;
- c = cohesion;
- G = slip-line geometry similitude factor;
- CI = cone index, defined (in psi) as the penetration resistance/A_o where, in this study, the resistance at 6-in. penetration is used as a reference;
- R_o = radius of cone base;
- w = surcharge;
- r, z = coordinates;
- z_o = depth to which base of cone has penetrated;
- α = apex angle of cone or cone angle;
- β = complement to apex semiangle;
- γ = unit weight of soil;
- δ = friction angle between cone and soil;
- θ = angle between r-axis and major principal stress;
- φ = angle of internal friction of soil;
- ψ = $c \cot \varphi$;
- μ = $\pi/4 - \varphi/2$; and
- σ = $(\sigma_1 + \sigma_3)/2 + \psi$ (in general).

FORMULATION

The following set of differential equations represents the theoretically rigorous formulation to the problem of determining axially symmetric plastic stress states and slip-line fields:

$$d\sigma \pm 2\sigma \tan \phi d\theta - (\gamma/\cos \phi) [\sin(\pm\phi)dr + \cos(\pm\varphi)dz] + (\sigma/r) [\sin \phi dr \pm \tan \phi(1 - \sin \phi)dz] = 0$$

$$dz = dr \tan(\theta \pm \mu) \tag{1}$$

This set of equations is obtained by combining the equations of equilibrium derived from plasticity theory with the Coulomb failure criterion. The circumferential stress is assumed to be the intermediate principal stress and to be equal to the minor principal stress σ_3. The r-axis of the coordinate system is parallel to the ground surface, and the positive z-axis is perpendicular to it into the soil mass (Fig. 1). The upper sign refers to the family of slip lines corresponding to the first characteristics of the differential equations (i-lines), and the lower sign refers to the second (j-lines).

No closed-form solution to these equations exists. Several numerical solutions have been presented; however, these are restricted to the axially symmetric surface loading of the semi-infinite half space. The equations given below are the numerical form of Eq. 1 and are used to study the effect of soil properties and cone parameters on the penetration characteristics of a right circular cone penetrating soil. So that the problem can be kept perfectly general, soil body forces have been included in the formulation. For a given set of loading conditions w over the horizontal soil surface, the values of $r_{i,j}$, $z_{i,j}$, $\sigma_{i,j}$, and $\theta_{i,j}$ are computed for an adjacent nodal point (slip-line intersection point, Fig. 1) by use of the set of recurrence relations.

$$r_{i,j} = (z_{i-1,j} - z_{i,j-1} + \epsilon_1 r_{i,j-1} - \epsilon_2 r_{i-1,j})/(\epsilon_1 - \epsilon_2) \tag{2}$$

$$z_{i,j} = z_{i-1,j} + (r_{i,j} - r_{i-1,j})\epsilon_2 \tag{3}$$

where $r_{i,j}$ and $z_{i,j}$ are the coordinates of the adjacent nodal point, $\epsilon_1 = \tan(\theta_{i,j-1} + \mu)$, and $\epsilon_2 = \tan(\theta_{i-1,j} - \mu)$. With these values of $r_{i,j}$ and $z_{i,j}$, the computation is continued.

$$\sigma_{i,j} = \{2\sigma_{i-1,j}\sigma_{i,j-1}[1 + \tan\varphi(\theta_{i,j-1} - \theta_{i-1,j})] + \sigma_{i-1,j}D + \sigma_{i,j-1}C - \sigma_{i,j-1}\sigma_{i-1,j}(B/r_{i,j-1} + A/r_{i-1,j})\}/(\sigma_{i,j-1} + \sigma_{i-1,j}) \tag{4}$$

$$\theta_{i,j} = [\sigma_{i,j-1} - \sigma_{i-1,j} + 2\tan\varphi(\sigma_{i,j-1}\theta_{i,j-1} + \sigma_{i-1,j}\theta_{i-1,j}) + D - C + \sigma_{i-1,j}A/r_{i-1,j} - \sigma_{i,j-1}B/r_{i,j-1}]/2\tan\varphi(\sigma_{i,j-1} + \sigma_{i-1,j}) \tag{5}$$

where

$A = \sin\varphi(r_{i,j} - r_{i-1,j}) - \tan\varphi(1 - \sin\varphi)(z_{i,j} - z_{i-1,j})$;
$B = \sin\varphi(r_{i,j} - r_{i,j-1}) + \tan\varphi(1 - \sin\varphi)(z_{i,j} - z_{i,j-1})$;
$C = \gamma[z_{i,j} - z_{i-1,j} - \tan\varphi(r_{i,j} - r_{i-1,j})]$; and
$D = \gamma[z_{i,j} - z_{i,j-1} + \tan\varphi(r_{i,j} - r_{i,j-1})]$.

To apply these recurrence relations to the problem of cone indentation required that the geometric boundary conditions as well as the stress boundary conditions be formulated appropriately and included in the computer program. The geometric boundary conditions are simply mathematical descriptions of the cone geometry and its position at depth in terms of r, z, α, and R_o. The stress boundary conditions and the method of computation are essentially the same as those described by the authors elsewhere for 2-dimensional conditions (1).

Briefly, the stress boundary condition on the horizontal plane through the base of the cone is given by the surcharge w and the overburden soil pressure (Fig. 1). Overburden shear is disregarded. The slip-line field in the passive zones is computed by Eq. 1 starting with these boundary values and an assumed value for the horizontal extent of the passive zone. In the radial shear zone, the same equations are used, but special consideration is given to the central point where the j-lines converge (point Q, Fig. 1). This point is a degenerated slip line, where θ changes from the value at the passive zone boundary to that specified at the active zone boundary. The total change in θ is divided by the number of slip lines converging at this point to obtain an equal $\Delta\theta$ increment between 2 adjacent slip lines. The σ values for each increment are computed

from the equation $\sigma = \sigma_o e^{2(\theta-\theta_o)\tan\phi}$, which is the solution to Eq. 1 if both dr and dz vanish. Allowance must be made for the angle β as well as δ when transition values of θ and σ are assigned between the active and passive zones. These values of θ and σ for each slip line at this point permit the coordinates as well as the σ and θ values for all other points in the radial shear zone to be computed by Eq. 1. In the active zone, the same equations are used, except for the points at the loaded surface of the cone itself, where $\theta_{1,j}$ is assigned and $z_{1,j} = z_o + (R_o - r_{1,j}) \tan \alpha$. Here,

$$r_{1,j} = \{r_{1-1,j} \tan[(\theta_{1,j} + \theta_{1-1,j})/2 - \mu] - z_{1-1,j} + R_o \tan \alpha + z_o\}/$$
$$\{\tan[(\theta_{1,j} + \theta_{1-1,j})/2 - \mu] + \tan \alpha\} \quad (6)$$

and

$$\sigma_{1,j} = \sigma_{1-1,j} + \sigma_{1-1,j}(\theta_{1,j} - \theta_{1-1,j}) \tan \varphi + C - [(\sigma_{1-1,j}A)/(r_{1-1,j})] \quad (7)$$

The numerical computation is performed and adjustments are made, if necessary, to the value assumed for the horizontal extent of the passive zone until the slip-line field "closes" on the axis of symmetry at the apex of the cone.

RESULTS AND CONCLUSIONS

Theoretical Results

The numerical computation of the slip-line field geometries and associated stresses by the recurrence relations (Eqs. 2 through 5) was performed on an Adage, Inc., time-sharing computer system. This system is based on Digital Equipment Corporation PDP-10 processors. To show specifically the effect of cone angle on the slip-line field geometry, we solved the governing differential equations for a set of ideal soil conditions that describe a homogeneous, dry, and purely frictional sand. These conditions are $c = 0$, $\varphi = 37$ deg, $\gamma = 100$ pcf, $w = 1$ psf, and $\delta = 20$ deg. The numerical results were plotted automatically and electronically on the display tube of a Computer Displays, Inc., advanced remote display system. The slip-line fields for $R_o = 0.034$ ft (radius of the Waterways Experiment Station cone) and $\alpha = 15.5$, 30, 60, 90, 120, and 150 deg have been reproduced and are shown in Figure 2. Because the problem is axially symmetric, only half of the total field has been shown; the dashed line indicates the central axis of the cone. The geometric scale may be obtained for each figure from the knowledge that the base radius of the cone is 0.4 in. The scale shown in Figure 2a is 4 times that shown in Figure 2b.

For given soil strength parameters c and φ, the slip-line fields representing the solution of the differential equations are geometrically similar only if the ratio $G = \gamma\ell/(c + w \tan \varphi)$ is the same (3), where ℓ is a characteristic length usually taken equal to R_o. Although the slip-line geometry similitude factor G, as defined by Cox for the case of bearing capacity, is the same (4.512) in all of the cases shown in Figure 2, it is obvious that the slip-line geometries differ—an indication that the G-equality is a necessary but not sufficient condition for slip-line field similitude. In addition to G, there must also be equality in δ and a similitude in the geometric condition at both the free and loaded boundaries to obtain complete geometric similitude of the slip-line field.

Figure 2 distinctly shows a contraction of the radial shear zone with decrease in cone angle. The contraction is so pronounced (Fig. 2b) that the individual i- and j-lines are hardly discernible with the scale used. The active, passive, and radial shear zones all have curvilinear boundaries because of the 3-dimensional nature of the problem, an indication that the geometries obtained from the solution of the theoretically correct differential equations differ from those obtained by using the Prandtl solution for weightless soil and the log-spiral approximation in the radial zone.

Figure 2 also shows that, with decreasing cone angle, the affected volume of soil increases. For the soil and cones used, the volume of the body of revolution formed by the slip-line field for $\alpha = 30$ deg is about 10 times greater than that for $\alpha = 150$ deg.

For compressible soils, the size of the affected mass directly influences the load-penetration relation. The material must be compressed to a state in which friction is fully mobilized before shear failure along slip lines can take place. The load necessary to accomplish this compression is usually less than the load needed to fail the soil in shear. It follows that the larger the volume of the slip-line field is, the more the soil mass must be compressed to mobilize the friction fully. Therefore, cone indexes obtained with cone shapes that result in large-volume slip-line fields are likely to be less representative of the Coulombic strength than of the compressibility of the material.

Experimental Results

A series of penetration tests was conducted on Jones Beach sand by using aluminum cones. The friction angle between the aluminum surface of the cone and the sand was assumed to be uniform and equal to 15 deg on the basis of experiments performed by Mohr and Karafiath (16). The purpose of the tests was to determine the effect of cone angle α on the value of the cone index CI. The base area of cones having apex angles of 150, 90, and 30 deg was 0.5 in.^{2}. The 30-deg cone corresponds to the Waterways Experiment Station cone. Also used was a cone having a base area of 1.04 in.^{2} and an apex angle of 15.5 deg. This cone corresponds to that used until 1956 by the North Dakota State Highway Department for flexible pavement design. The ranges of φ over normal stress levels of interest for ranges of γ obtained from triaxial tests on Jones Beach sand were as follows:

γ (pcf)	φ (deg)
103.5 to 105.5	41 to 37
95.5 to 97.5	38 to 30

Uniform soil beds were prepared to a narrow range of desired densities in a facility specially designed for this purpose.

The cones were attached interchangeably to a 12-in. rod, and the entire assembly was mounted on the loading frame of an Instron testing instrument model TM-M (Fig. 3). The rate of penetration was set at 10 cm/min. Load-penetration curves were obtained automatically on a synchronized strip-chart recorder. Values of CI as defined for this study were determined directly from the load-penetration curves. The results of the penetration test series are shown in Figures 4 and 5.

Figure 4 shows the variation of cone index with change in cone angle for Jones Beach sand at various relative densities, as follows:

Density	Dγ	γ (pcf)
Dense	67 to 100	100 to 107
Medium	34 to 66	94 to 100
Loose	<34	88 to 94

It is clear from the figure that when the material is loose the cone angle has very little effect on the cone index (all values of CI are less than approximately 9 regardless of the size of the cone angle). On the other hand, for dense materials, CI varies from approximately 19 for the 15.5-deg cone to between 44 and 60 for the 150-deg cone. These results seem to verify the previously discussed effect of compressibility on the value of cone index. Apparently the frictional strength of the loose material cannot be fully mobilized until the material is sufficiently compressed to allow for complete shear failure. Calculations made on the basis of volume-change properties of the Jones Beach sand indicated that the average percentage of volume change of the soil mass within the slip-line field was virtually independent of the apex angle of cones having the same base area. Consequently, the displacement necessary to mobilize the full friction is roughly proportional to the volume of the slip-line field. These results suggest that, in order for the cone index to be used as a valid measure of the frictional strength of a soil, 2 cones should be used, both having the same base area but one having an obtuse apex angle and the other an acute apex angle. If the values of CI obtained from these 2 cones are similar, then the penetration resistance is governed by the

Figure 1. Geometry for cone indentation problem (boundary conditions and slip lines are symmetric with z-axis).

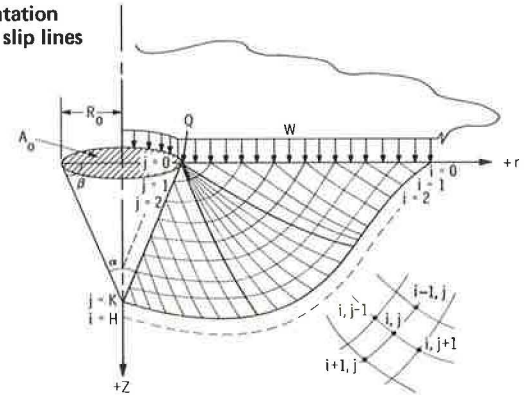

Figure 2. Slip-line fields for cones penetrating ideal soil.

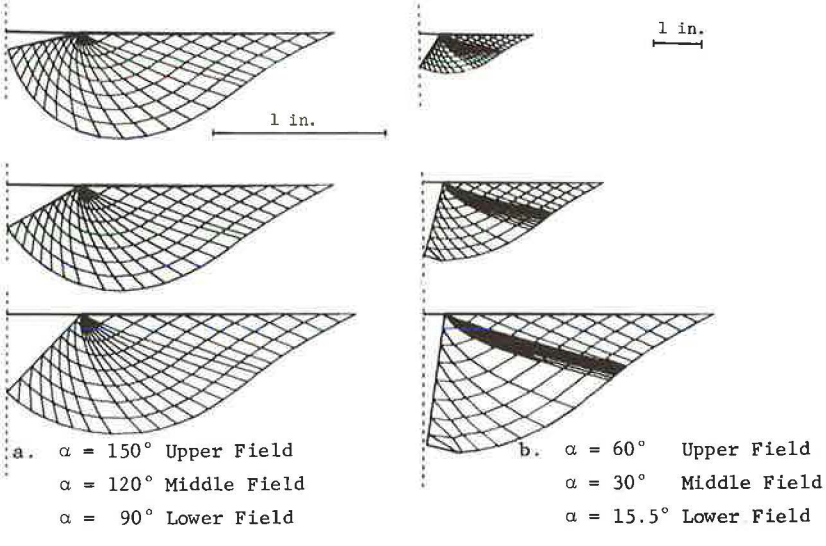

Figure 3. Loading and recording equipment for cone penetrometer test.

Figure 4. Cone index at 6-in. penetration versus cone angle for Jones Beach sand at various relative densities.

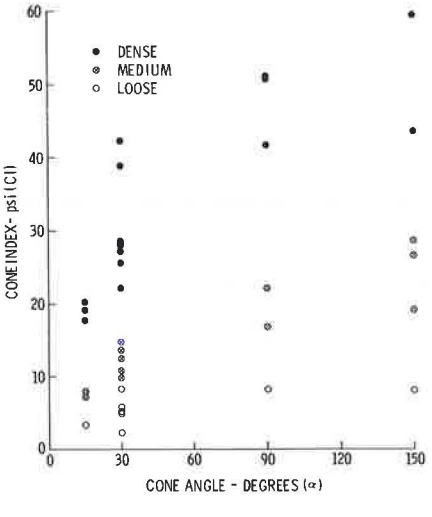

Figure 5. Cone index at 6-in. penetration versus unit weight for cones having different apex angles.

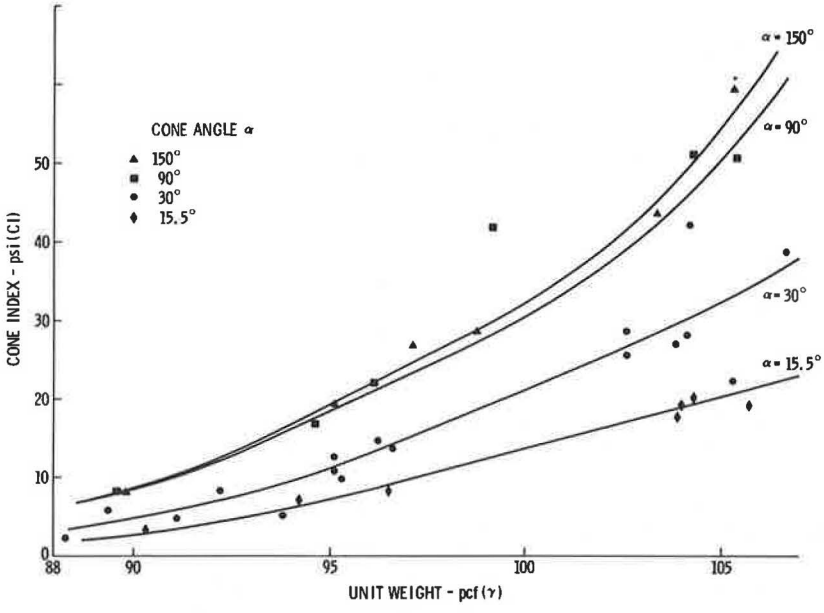

Figure 6. Cone index at 6-in. penetration versus unit weight for 150 deg.

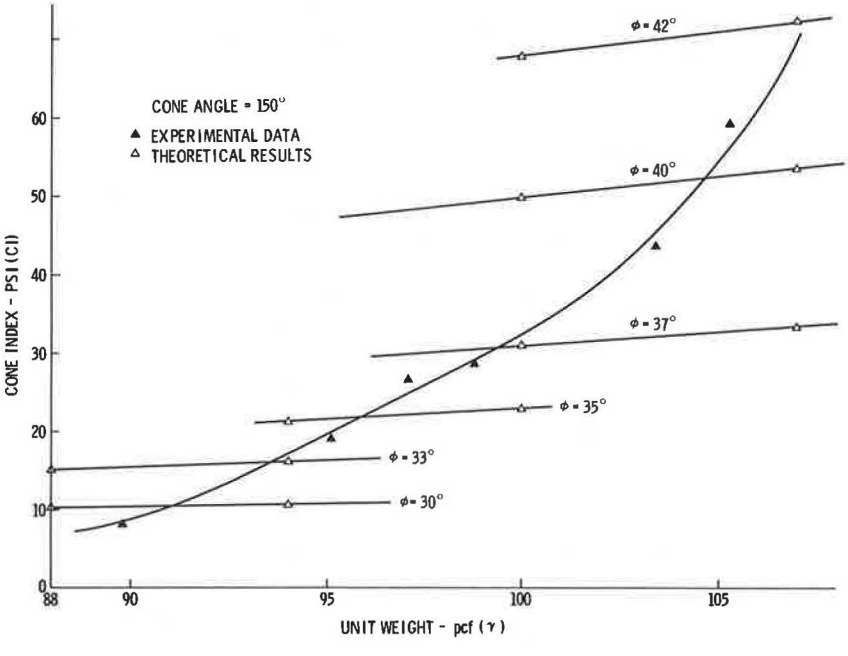

compressibility of the soil. If, on the other hand, the 2 values are markedly different, then a relation may properly be sought between CI and the strength parameters of the material.

Of course, the problem is not entirely that simple. In addition to the compressibility effect at lower relative densities, there is the effect of the variation of φ with γ. Figure 5 shows for each of the cones investigated the change in cone index with variation of unit weight. It is impossible from such a plot to distinguish which of the 2 effects has the greater influence. However, it seems reasonable to assume that, in the range of unit weights over which the material may be considered relatively dense, the compressional effect is negligible.

Comparison of Experimental and Theoretical Results

Figure 6 shows a comparison of the experimentally obtained values of CI over a wide range of unit weights with the values determined theoretically by the solution of the differential equations of plastic equilibrium. For clarity, only the results for the 150-deg cone are presented. The theoretical curves suggest that for φ constant there is little change in CI with variation in γ. The theoretical curves also show that for a given unit weight the value of CI is very sensitive to changes in φ. The experimental curve, which shows a pronounced decrease of CI with decrease in γ, not only reflects the change in φ with unit weight and stress level but also includes the effect of soil compressibility discussed above. Unfortunately, the experimental curve itself does not distinguish between these effects; however, for reasons cited above, it seems that the compressibility has the least influence on tests performed with dense material. For example, a cone index of 43 for Jones Beach sand at 103 pcf indicates a φ-angle of approximately 38 to 39 degrees (Fig. 6). For the stress level involved, this value of φ determined from cone penetrometer data agrees quite well with the values obtained from triaxial tests on Jones Beach sand.

Therefore, although the theory of plastic equilibrium has not been modified in this study to include in the computation of CI the effects of a curvilinear Mohr envelope (2, 17) or the contribution of soil compressibility, we believe that curves such as those shown in Figure 6 can be used to estimate an average value of φ from cone penetrometer data.

SUMMARY AND DISCUSSION

1. For the axially symmetric case, the slip-line field geometry derived from the theory of plastic equilibrium for a dry, uniform sand being penetrated by a cone differs markedly from that obtained by the Prandtl solution for weightless soil and the log-spiral approximation.
2. For materials at high relative densities, the cone index varies significantly with the size of the penetrometer apex angle, all other conditions being equal. This is not observed for loose materials. Soil compressibility, the variation of φ with γ, and the curvilinear nature of the Mohr failure envelope can account for this difference in performance.
3. Solutions derived from the theory of plastic equilibrium agree well with experimentally obtained cone penetrometer data and can be used, under certain conditions, to estimate the strength parameter φ for a dense dry sand. In all penetrometer investigations, the use of 2 cones is recommended to avoid misinterpretation of the cone index. One cone should have an obtuse apex angle, the other an acute angle.

Further investigations are needed to enhance the theory presented in this study. For example, it would be very desirable to incorporate into the computer program the curvilinearity of the Mohr envelope and the dependence of φ on unit weight. Similarly, the effect of compressibility on the penetration resistance of a material should be expressed quantitatively, and criteria for the mobilization of friction in the slip-line field should be established.

REFERENCES

1. Berezantzev, V. G. Certain Results of Investigation on the Shear Strength of Sands. Proc., Geotechnical Conf., Oslo, Vol. 1, 1967, pp. 167-169.
2. Berezantzev, V. G., and Kovalev, I. V. Consideration of the Curvilinearity of the Shear Graph When Conducting Tests on Model Foundations. Osnovaniya, Fundamenty i Mekhanika Gruntov, No. 1, 1968, pp. 1-4 (trans.).
3. Cox, A. D. Axially-Symmetric Plastic Deformation in Soils—II: Indentation of Ponderable Soils. Internat. Jour. of Mechanical Sciences, Vol. 4, 1962, pp. 371-380.
4. Cox, A. D., Eason, G., and Hopkins, H. G. Axially-Symmetric Plastic Deformation in Soils. Trans., Royal Soc., London, Series A, Vol. 254, 1961, pp. 1-45.
5. Drucker, D. C., and Prager, W. Soil Mechanics and Plastic Analysis or Limit Design. Quarterly of Applied Mathematics, Vol. 10, No. 2, 1952, pp. 157-165.
6. Fletcher, G. The Standard Penetration Test: Its Uses and Abuses. Jour. Soil Mech. and Found. Div., Proc. ASCE, Vol. 91, No. SM4, 1965, pp. 67-76.
7. Karafiath, L. L., and Nowatzki, E. A. Stability of Slopes Loaded Over a Finite Area. Highway Research Record 323, 1970, pp. 14-25.
8. Larkin, L. A. Theoretical Bearing Capacity of Very Shallow Footings. Jour. Soil Mech. and Found. Div., Proc. ASCE, Vol. 94, No. SM6, 1968, pp. 1347-1357.
9. Meyerhof, G. G. Penetration Tests and Bearing Capacity of Cohesionless Soils. Jour. Soil Mech. and Found. Div., Proc. ASCE, Vol. 82, No. SM1, 1956, pp. 1-19.
10. Meyerhof, G. G. The Ultimate Bearing Capacity of Wedge-Shaped Foundations. Proc., Fifth Internat. Conf. on Soil Mech. and Found. Eng., Paris, Vol. 2, 1961, pp. 105-109.
11. Mohr, G., and Karafiath, L. L. Determination of the Coefficient of Friction Between Metals and Nonmetals in Ultrahigh Vacuum. Research Department, Grumman Aerospace Corp., Rept. RE-311, Dec. 1967.
12. Prandtl, L. Ueber die Harte plastischer Korper. Gottingen Nachr., Math Phys. Kl., 1920, p. 74.
13. Schultz, E., and Knausenberger, H. Experiences With Penetrometers. Proc., Fourth Internat. Conf. on Soil Mech. and Found. Eng., Vol. 1, 1957, pp. 249-255.
14. Sneddon, I. N. The Relation Between Load and Penetration in the Axisymmetric Boussinesq Problem for a Punch of Arbitrary Profile. Internat. Jour. of Engineering Science, Vol. 3, 1965, pp. 47-57.
15. Sokolovskii, V. V. Statics of Granular Media. Pergamon Press, 1965.
16. Spencer, A. J. M. Perturbation Methods in Plasticity—III: Plane Strain of Ideal Soils and Plastic Solids With Body Forces. Jour. of Mechanics and Physics of Solids, Vol. 10, 1962, pp. 165-177.
17. Szymanski, C. Some Plane Problems of the Theory of Limiting Equilibrium of Loose and Cohesive, Non-Homogeneous Isotropic Media in the Case of a Non-Linear Limit Curve. In Non-Homogeneity in Elasticity and Plasticity (Olszak, W., ed.), Pergamon Press, 1958.
18. Soil Properties in Vehicle Mobility Research: Measuring Strength-Density Relations of an Air-Dry Sand. U. S. Army Engineer Waterways Experiment Station, Corps of Engineers, Vicksburg, Miss., Tech. Rept. 3-652, Aug. 1964.